Anal. Chem. **2005,** *77,* 4293−4299

Accelerated Articles

Million-fold Preconcentration of Proteins and Peptides by Nanofluidic Filter

Ying-Chih Wang,[†,‡] Anna L. Stevens,[§] and Jongyoon Han*[,‡,§]

Department of Mechanical Engineering, Biological Engineering Division, and Department of Electrical Engineering and Computer Science, Massachusetts Institute of Technology, Cambridge, Massachusetts 02139

We have developed a highly efficient microfluidic sample preconcentration device based on the electrokinetic trapping mechanism enabled by nanofluidic filters. The device, fabricated by standard photolithography and etching techniques, generates an extended space charge region within a microchannel, which was used to both collect and trap the molecules efficiently. The electrokinetic trapping and collection can be maintained for several hours, and concentration factors as high as 10^6-10^8 have been demonstrated. This device could be useful in various bioanalysis microsystems, due to its simplicity, performance, robustness, and integrabilty to other separation and detection systems.

One of the major challenges of proteomics is the sheer complexity of biomolecule samples, such as blood serum or cell extracts. Typical blood samples can contain more than 10 000 different protein species, with concentrations varying over 9 orders of magnitude.[1] Such diversities of proteins, as well as their huge concentration ranges, pose a formidable challenge for sample preparation in proteomics. Conventional protein analysis techniques, based on multidimensional separation steps and mass spectrometry, fall short because of the limited separation peak capacity (up to ∼3000) and dynamic range of detection (∼10^4).[2]

Microfluidic biomolecule analysis systems promise to be the enabling technology for automated biomolecule processing.[3,4] Various biomolecule separation and purification steps, as well as chemical reactions and amplifications, have been miniaturized on microchips. These achievements demonstrate sample processing and separations that are a 100-fold faster than current methods. In addition, microfluidic integration of two different separation steps into a multidimensional separation device has been demonstrated.[5−8]

However, most microfluidic separation and sample processing devices suffers from the critical scaling problems. Microfluidic devices are efficient in handling and processing 1pL−nL of sample fluids, but most biomolecule samples are available or handled in a liquid volume larger than 1 μL. Therefore, microchip-based separation techniques often analyze only a small fraction of available samples, which could limit the overall detection sensitivity, especially for the detection of low-concentration species in the sample. In proteomics, this problem is exacerbated by the fact that information-rich signaling molecules, for example, cytokines and biomarkers, are present only in trace concentrations (nM−pM range). Furthermore, there is no signal amplification technique, such as polymerase chain reaction (PCR), for proteins and peptides.

What is critically needed is an efficient sample concentrator that can take typical microliter or more sample volumes and concentrate molecules into a smaller volume so that samples can be separated and detected much more sensitively. Several strategies are currently available to provide sample preconcentration in liquids, including field-amplified sample stacking (FAS),[9]

* Corresponding author: (e-mail) jyhan@mit.edu.
† Department of Mechanical Engineering.
‡ Department of Electrical Engineering and Computer Science.
§ Biological Engineering Division.

(1) Rabilloud, T. *Proteomics* **2002**, *2*, 3−10.
(2) Hamdan, M.; Righetti, P. G. *Mass Spectrom. Rev.* **2003**, *22*, 272−284.
(3) Auroux, P.-A.; Iossifidis, D.; Reyes, D. R.; Manz, A. *Anal. Chem.* **2002**, *74*, 2637−2652.
(4) Reyes, D. R.; Iossifidis, D.; Auroux, P.-A.; Manz, A. *Anal. Chem.* **2002**, *74*, 2623−2636.
(5) Rocklin, R. D.; Ramsey, R. S.; Ramsey, J. M. *Anal. Chem.* **2000**, *72*, 5244−5249.
(6) Herr, A. E.; Molho, J. I.; Drouvalakis, K. A.; Mikkelsen, J. C.; Utz, P. J.; Santiago, J. G.; Kenny, T. W. *Anal. Chem.* **2003**, *75*, 1180−1187.
(7) Li, Y.; Buch, J. S.; Rosenberger, F.; DeVoe, D. L.; Lee, C. S. *Anal. Chem.* **2004**, *76*, 742−748.
(8) Wang, Y.-C.; Choi, M. H.; Han, J. *Anal. Chem.* **2004**, *76*, 4426−4431.
(9) Burgi, D. S.; Chien, R.-L. *Anal. Chem.* **1991**, *63*, 2042−2047.

10.1021/ac050321z CCC: $30.25
Published on Web 06/10/2005

isotachophoresis,[10] electrokinetic trapping,[11,12] micellar electrokinetic sweeping,[13] chromatographic preconcentration,[14,15] and membrane preconcentration.[16,17] Many of these techniques were originally developed for capillary electrophoresis (CE) and require special buffer arrangements, reagents, or both. The efficiency of chromatographic and filtration-based preconcentration techniques depends on the hydrophobicity and the size of the target molecules. Electrokinetic trapping can be used for any charged biomolecule species, but generally such techniques require nanoporous charge-selective membranes for the operation. Overall, the demonstrated concentration factors for the existing preconcentration schemes in the microchips are limited to 1000-fold, and their coupling with integrated microsystems is difficult due to various operational constraints, such as reagent and material requirements.

To solve these problems, we have developed a novel microfluidic sample concentration system based on electrokinetic trapping and nonlinear electroosmotic flow in a chip. The device can be fabricated using the standard microfabrication techniques and does not require any special reagents or membrane materials. Instead of charge-selective nanoporous membranes, regular, flat nanofluidic filters filled with buffer solution are used as an ion-selective membrane to generate an ion-depletion region for electrokinetic trapping. The device collects charged biomolecules efficiently because of two main features: (1) the energy barrier for charged biomolecules generated by the induced space charge layer near the nanofluidic filter; (2) a faster nonlinear electroosmotic flow for sample deliveries driven by the induced space charge in the microchannel. The combination of these two phenomena results in a rapid preconcentration of proteins and peptides within a microfluidic channel, without any physical barriers or reagents, up to 10^6-10^8 fold in concentration. Preconcentration experiments of proteins and peptides show that the preconcentration operation is possible over several hours, which allows extremely high preconcentration factors.

EXPERIMENTAL SECTION

Chip Fabrication. The details about fabrication techniques are available elsewhere.[18,19] The devices were fabricated by standard photolithography and reactive ion etching (RIE) on silicon wafers, followed by wafer bonding to seal the microfluidic channels. After patterning the 5−20-μm-wide nanochannels with standard lithography tools, the wafer was etched for ~10 s to a depth of 40 nm. Then the second photolithography and etching step made two parallel 1.5-μm microfluidic channels across the nanochannels (nanofilters). After the RIE etching, KOH etching was used to etch through the loading holes. Then, thermal oxidation was done after the nitride stripping to provide proper electrical insulation. The bottom side was then bonded with a Pyrex wafer using anodic bonding techniques. Nanofilters with a depth between 30 and 70 nm were fabricated to demonstrate the effects of buffer concentration and channel depth.

Material and Reagents. The buffer, 10 mM phosphate (dibasic sodium phosphate) at pH 9.1 was mainly used, with 10 μM EDTA to prevent bacterial growth. Successful preconcentration was demonstrated also at pH 4.6, 10 mM phosphate buffer. In addition, 10 mM pH 3.5 acetate buffer and 1× TBE buffer (~80 mM) were tested, but without significant preconcentration effect.

The molecules and dyes used in this work were rGFP (BD bioscience, Palo Alto, CA), FITC−BSA (Sigma-Aldrich, St. Louis, MO), FITC−ovalbumin (Molecular Probes, Eugene, OR), FITC dye (Sigma-Aldrich), Mito Orange (Molecular Probes), and λ-DNA (500 μg/mL). DNA molecules were labeled with YOYO-1 intercalating dyes (Molecular Probes) following the manufacturer's instruction.

The peptide (NH_2−GCEHH−COOH, p*I* 4.08) molecules were synthesized at the Biopolymers Lab at MIT and labeled with a thiol-conjugating dye using the following procedure. The HPLC-purified peptide sample was first reconstituted into a 10 mM peptide concentration in 0.1 M pH 7.4 phosphate buffer as a stock solution and then was diluted to 1 mM. The diluted stock solution was mixed in a 1:1 ratio with 10 mM TCEP (Molecular Probes) and then with 5-TMRIA dye (Molecular Probes). The reaction was allowed to proceed in the refridgerator for 24 h, shielded from light. At the end, nonreacted dyes were terminated by adding 100 mM 2-mercaptoethanol (Sigma-Aldrich) and filtered out from the peptide sample using a minidialysis kit with a 1-kDa cutoff (Amersham Bioscience, Piscataway, NJ).

In-gel digestion extractions from a polyacrylamide gel slice were used as buffer additives in one of the experiments. This is to simulate the situation of using biosamples in the preconcentration device directly from gel electrophoresis as in typical proteomics research environments. The extract solution contains no proteins, but small amounts of salts and small molecules may be present in the gel from the sample or electrophoresis buffer (Tris, glycine, sodium dodecyl sulfate, glycerol, dithiothreitol, possible keratin contaminants), from staining (coomassie blue), or from the reduction and alkylation steps (tris(2-carboxyethyl)-phosphine hydrochloride, iodoacetamide, ammonium bicarbonate). The extraction by sonication was performed on the trypsinization solution (60 μL; 10 ng/μL trypsin, trypsin peptides, or both in ammonium bicarbonate buffer) following enzyme inactivation with 20 μL of 20% formic acid. This extraction solution was collected and concentrated in the Speedvac. Extraction with sonication was performed sequentially using 200 μL of 100 mM ammonium biocarbonate, 0.1% trifluoroacetic acid (TFA) in water, and 0.1% TFA in 50:50 water to acetonitrile twice. Each time the extracted solution was collected, pooled with the extracted solution from the preceding step, and concentrated down to ~10 μL in the Speedvac.

Optical Detection Setup. All the experiments were imaged with an inverted epifluorescence microscope (IX-71), which has a built-in 100-W mercury lamp and a standard FITC filter set (Olympus, Melville, NY). In these experiments, a thermoelectrically cooled CCD camera (Cooke Corp., Auburn Hill, MI) was

(10) Gebauer, P.; Bocek, P. *Electrophoresis* **2002**, *23*, 3858−3864.
(11) Astorga-Wells, J.; Swerdlow, H. *Anal. Chem.* **2003**, *75*, 5207−5212.
(12) Singh, A. K.; Throckmorton, D. J.; Kirby, B. J.; Thompson, A. P. *Micro Total Anal. Syst.* **2002**, 347−349.
(13) Quirion, J. P.; Terabe, S. *Science* **1998**, *282*, 465−468.
(14) Oleschuk, R. D.; Shultz-Lockyear, L. L.; Ning, Y.; Harrison, D. J. *Anal. Chem.* **2000**, *72*, 585−590.
(15) Yu, C.; Davey, M. H.; Svec, F.; Frechet, J. M. J. *Anal. Chem.* **2001**, *73*, 5088−5096.
(16) Song, S.; Singh, A. K.; Kirby, B. J. *Anal. Chem.* **2004**, *76*, 4587−4592.
(17) Khandurina, J.; Jacobson, S. C.; Waters, L. C.; Foote, R. S.; Ramsey, J. M. *Anal. Chem.* **1999**, *71*, 1815−1819.
(18) Han, J.; Craighead, H. G. *Science* **2000**, *288*, 1026−1029.
(19) Han, J.; Craighead, H. G. *J. Vacuum Sci. Technol., A* **1999**, *17*, 2142−2147.

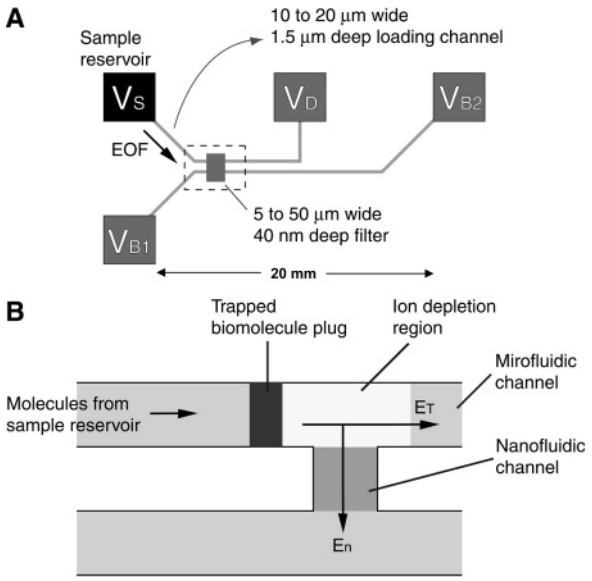

Figure 1. Nanofluidic protein concentration device: (A) The layout of the device. (B) Schematic diagram that shows the concentration mechanism. Once proper voltages are applied, the trapping region and depletion region will be formed as indicated in the drawing. The E_T specifies the electrical field applied across the ion depletion region, while the E_n specifies the cross nanofilter electrical field.

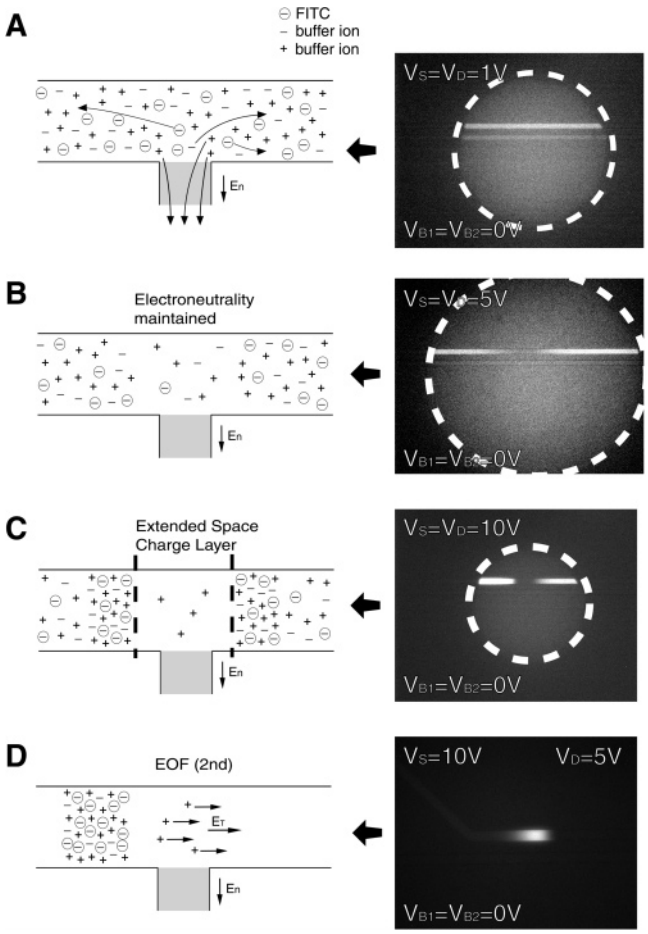

Figure 2. Mechanism of preconcentration in the nanofilter device (A) No concentration polarization is observed when a small electrical field (E_n) is applied across the nanofilter. (B) As the E_n increases, the transport of ions becomes diffusion-limited and generates the ion-depletion zone. However, the region maintains its electroneutrality. (C) Once a strong field (E_n) is applied, the nanochannel will develop an induced space charge layer, where electroneutrality is no longer maintained. (D) By applying an additional field (E_T) along the microfluidic channel in the anodic side (from V_S to V_D), a nonlinear electrokinetic flow (called electroosmosis of the second kind) is induced, which results in fast accumulation of biomolecules in front of the induced space charge layer.

used for fluorescence imaging. Sequences of images were analyzed by IPLab 3.6 (Scanalytics, Fairfax, VA). A homemade voltage divider was used to distribute different potentials to reservoirs. In addition, to prevent CCD array from being saturated by highly concentrated peaks, a neutral density filter was used to reduce the excitation light intensity.

Quantification of Molecular Concentration. A highly concentrated plug of fluorescent molecules often saturated the CCD array, which will lead to errors in quantification. To increase the dynamic range of the detection and reduce the rate of photobleaching, the excitation light intensity was decreased by 3 orders of magnitude using a neutral density filter and aperture. The concentrated peak intensities were mapped with nondiluted 3.3 and 0.33 μM GFP samples. During the experiment, the molecules were not exposed to light, and the shutter was opened only during periodical exposures (~1 s) to minimize photobleaching of the collected molecules.

Nonspecific binding of proteins can be a problem, especially when a sample plug with a very high concentration is generated. Before and after each experiment, the detection area of the chip was exposed with an excess amount of laser light to completely quench any residual fluorescence due to the nonspecific binding of the fluorescent protein to the wall. Experiments were repeated with a freshly fabricated and filled device to eliminate any issues regarding the quantification of the molecular concentrations within the channel.

Device Layout. The schematic diagram of the device is shown in Figure 1. One or many thin nanofluidic channels, typically less than 50 nm in thickness, connect the two microfluidic channels. Two separate electric fields are applied and controlled independently, as shown in Figure 1B. The field in the nanofluidic channel (E_n) is used to generate the ion-depletion region and extended space charge layer that traps the biomolecules. The tangential field in the microfluidic channel (E_T), on the anodic side, is used to generate the electroosmotic flow to bring the molecules into the trapped region from the reservoir. The thickness and uniformity of the nanofluidic channel structure was checked by a scanning electron micrograph, and the fabrication technique we used produced a nanofluidic channel as thin as 20 nm, without significant deformation or collapsing of the channel.[20]

RESULTS AND DISCUSSION

Electrokinetic Trapping and Electroosmosis of the Second Kind Pumping. It has been previously reported that nanofluidic channels (~50 nm in thickness) can support ion-selective ion currents such as ion-exchange membranes.[21] When an electric

(20) Mao, P.; Han, J. Accepted for publication by *Lab on a Chip*.
(21) Petersen, N. J.; Dutta, D.; Alarie, J. P.; Ramsey, J. M. *Micro Total Anal. Syst.* **2004**, 348−350.

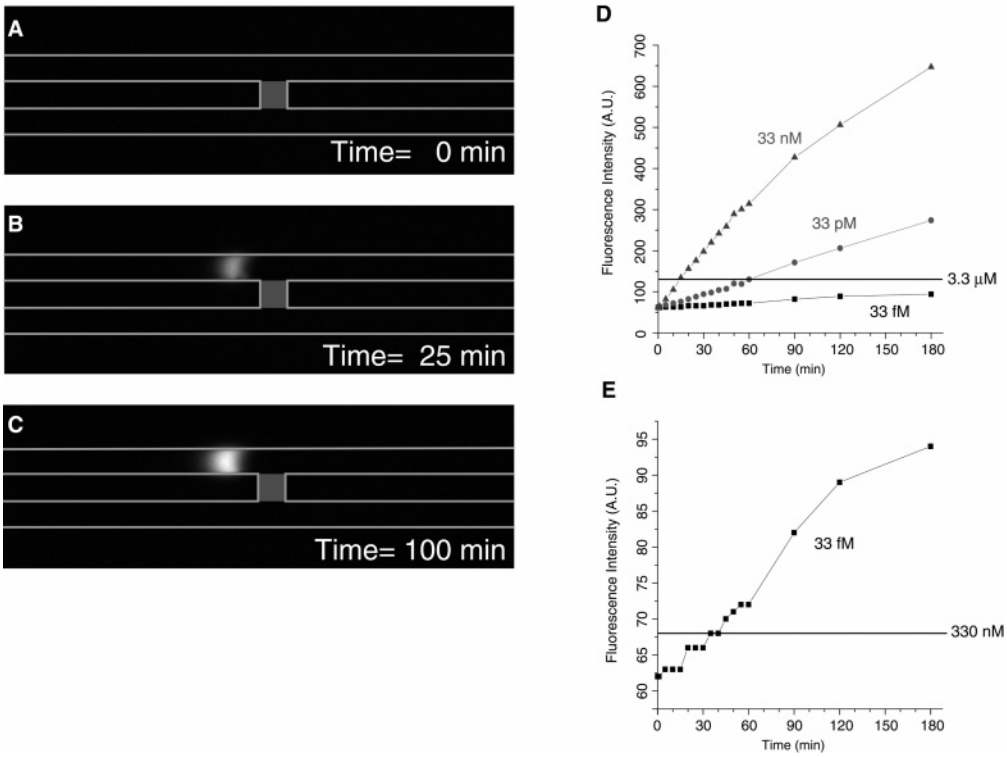

Figure 3. Preconcentration over 3 h with various sample concentrations. (A) Image of 33 pM GFP directly after loading the sample into the top microfluidic channel. (B) Iimage taken after applying $V_S = 10$ V, $V_D = 5$ V, and $V_{B1} = V_{B2} = 0$ V for 25 min. (C) Image taken after 100 min with the same potential values as (B). (D) Concentration of the collected GFP plug, starting from dilute GFP solutions with three different concentrations. (E) Closeup view for the 33 fM GFP experiment in (D). This shows at least a 10^7-fold concentration achieved within 40 min. The baseline shift (~62 arbitrary unit, AU) is the dark noise from the CCD camera.

field is applied across the nanofluidic channel, more counterions (from the Debye layer) than co-ions will migrate across it (Figure 2A). This results in net transfer of charges (counterions) from the anodic side to the cathodic side, and the overall ion concentration will be decreased on the cathodic side due to the concentration polarization effect (Figure 2B).[22,23] The ion depletion (caused by concentration polarization) near the nanofluidic channel will make the Debye layer thicker and overlap more significantly in the nanofluidic channel, which will speed up the concentration polarization. Above a certain threshold value of E_n, the ion transport across the channel enters a new, nonlinear regime (electrokinetics of the second kind), which has been previously reported in the ion-exchange membranes.[24,25] In this regime (Figure 2C), the counterions are depleted from the nanofluidic channel, and an extended space charge layer (induced electrical double layer) will be formed in the bulk solution nearby, within the microfluidic channel in this case.[25] Within this induced electrical double layer, electroneutrality is locally broken (these charges are screening the fixed surface charges within the nanochannel), and co-ions (biomolecules) are prohibited from this region because of its negative potential just as in the Debye layer. Such an induced mobile ion layer could generate a strong electroosmotic flow when a tangential component of electric field (E_T) is applied (Figure 2D). By carefully controlling the electric fields (E_n and E_T), one can balance the two forces (anion repulsion from the space charge layer versus electroosmotic flow from the reservoir), stabilizing the interface. At the interface, biomolecules coming from the sample reservoir can be continuously trapped and collected.

One of the notable characteristics of this nonlinear electroosmotic flow is that the flow velocity is a nonlinear function (in this case $\sim E_T E_n$) of the electric field. Therefore, they can generate much stronger electroosmotic flow velocity than the normal electroosmotic flow (caused by the surface Debye layer charges).[24] In previous experiments using charged membrane beads, electroosmosis of the second kind was shown to generate strong but uncontrollable flow vortices near the membrane,[24,26] which were used for a fast mixing. In these experiments, the electric field near the gel surface (where the induced space charge layer exists) is nonuniform, which leads to circulatory or chaotic flow vortices. We did observe similar oscillatory flow when the electric field values are not optimized to generate a stable boundary, which is required for preconcentration (see Supporting Information). However, under certain E_T/E_n ratios, the system will reach a steady state, where a stable virtual barrier is formed between extended space charge layer and normal fluid.

In this device, we achieve much better control on this phenomenon, for the following reasons: (1) The concentration

(22) Probstein, R. F. *Physicochemical Hydrodynamics: An Introduction*; Wiley-Interscience: New York, 1994.
(23) Madndersloot, W.; Hicks, R. E. *Ind. Eng. Chem. Process Des. Dev.* **1965**, *4*, 304.
(24) Mishchuk, N. A.; Takhistov, P. V. *Colloids Surf., A* **1995**, 119−131.
(25) Leinweber, F. C.; Tallarek, U. *Langmuir* **2004**, *20*, 11637−11648.
(26) Ben, Y.; Chang, H.-C. *J. Fluid Mech.* **2002**, *461*, 229−238.

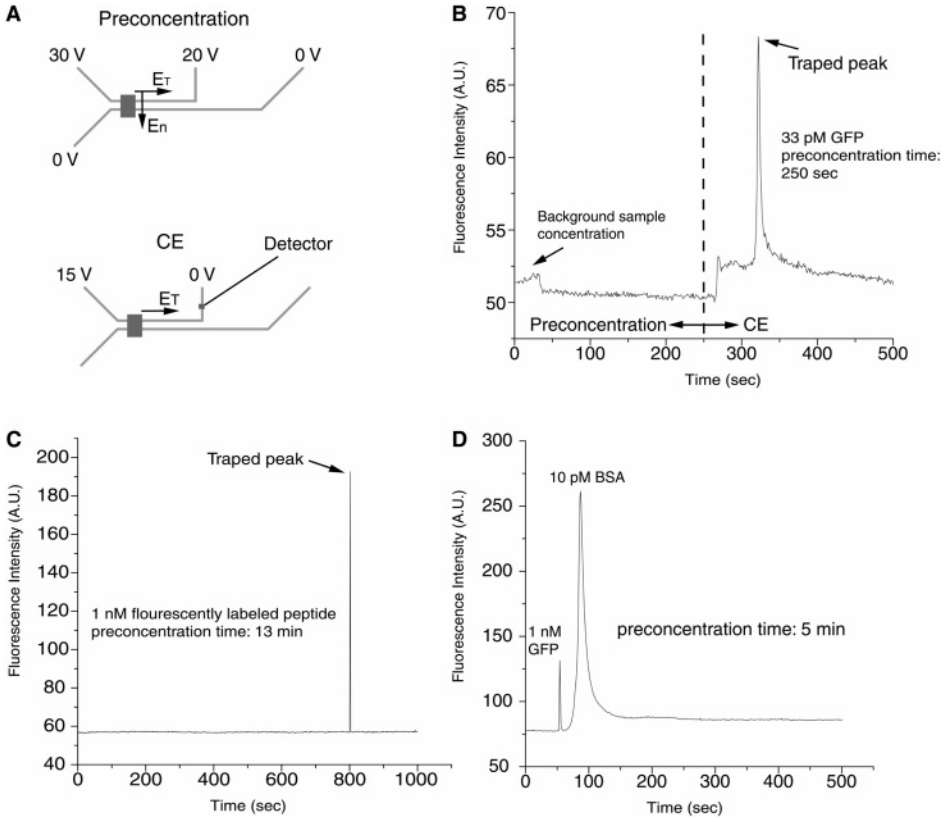

Figure 4. Release of collected biomolecules. (A) The schematic drawing shows the voltages applied to the reservoirs during the concentrating and release (on-chip free solution electrophoresis) steps. (B) From 0 to 250 s, the waste channel was grounded and a voltage is applied across the filter and triggers the trapping phenomena. As a result, the detector arranged downstream reads only the dark noise from the CCD array. The signal showing from 0 to 30 s comes from a 33 pM GFP solution exiting between the detector and nanofilter (~10 mm). To show each step in greater detail, all the detections in these cases were done without using a neutral density filter. Therefore, the picomolar-level GFP sample is in the detectable range. After 250 s, the waste channel was floated to release the collected molecules in the top channel. (C) Collection and release of fluorescently labeled peptide sample. An extremely sharp sample plug is formed, which saturates the CCD array used. (D) Capillary electrophoresis separation of two different proteins, co-collected for 5 min and released (launched). Unlike (B) and (C), where plots show both preconcentration and CE separation steps, (D) shows only the CE step.

polarization zone is confined in the microchannel, therefore creating a more uniform induced charge layer. (2) The tangential field (E_T) is uniform, unlike the gel experiment where the tangential field is determined by the curvature of the gel bead and very nonuniform. (3) Due to the small amount of current required and fast heat dissipation in the device, Joule heating is not a concern. (4) Unlike charged gels or membranes, nanofluidic channels do not swell or shrink depending on the ionic strength, temperature, or other environmental conditions, which is probably the reason for a long-term operation of the device. The concentration behavior in this system is different from that of FAS, since both anions and cations are collected in the concentration polarization zone.

Figure 3 demonstrates the performance of the preconcentration device over 3 h. In Figure 3A, 33 pM green fluorescent protein (GFP) sample solution was loaded into the sample reservoir, and the resulting trapped protein peaks were monitored by fluorescence microscopy (Figure 3B and 3C). The preconcentration of proteins can be stably maintained up to several hours, which allows for preconcentration factors of more than a million. Figure 3D and 3E show the preconcentration results of 33 nM, 33 pM, and 33 fM dilute GFP protein solutions monitored over ~3 h. The concentrations of collected GFP protein plugs were estimated by measuring the fluorescence signal from the molecules. The result shows that preconcentration factors of 10^6−10^8 have been achieved. The collection speed is decreased when the plug concentration became high (~1 μM), probably due to the excessive nonspecific binding of the protein on the channel surface.

One of the striking features of this preconcentration system is its speed. A 10^7-fold concentration has been achieved within 1 h. Since the approximate volume of concentrated plug is ~0.5 pL (~1.5 μm × 20 μm × 20 μm), this means the preconcentrator pumped sample liquid volume as large as 1 μL through the channel and trapped the GFP within that volume. Given the concentration time of ~10^4 s in this experiment, the average sample flow speed should be as high as 1 mm/s. This is not possible with normal electroosmotic flow (electroosmosis of the first kind), which only generates up to 10−100 μm/s with the field used in this experiment (~10 V/cm). The fast collection (and fast sample fluid pumping) can be explained only by the electroosmotic flow of the second kind. Induced space charges are generated within the microchannel by the field (E_n), and the tangential field (E_T) mobilizes these induced space charges toward the cathodic reservoir. Therefore, the preconcentrator presented not only traps the molecules but also pumps the sample liquid very efficiently. In addition to the sample preconcentration, this

device could be a novel, microfluidic fluid pumping device, which is much more efficient than electroosmotic (electrokinetic) pumping[27] and simpler to implement than ac electrokinetic pumping.[28,29]

Preconcentration in the Coated Channel. One major problem of protein analysis in untreated silica surfaces is the adsorption of samples. In this system, the adsorption can change the effective surface charge density and sometimes shift the optimal operating conditions. To eliminate this problem, a standard polyacryamide coating was used.[30] First, the device was coated with 3-(trimethoxysilyl)propyl methacrylate as an adhesion promoter. Then, 5% polyacrylamide solution was mixed with 0.2% VA-086 photoinitiator (WAKO, Richmond, VA) and exposed under a UV lamp for 5 min, to initiate polymerization. After the coating, there was no noticeable level of adsorption in the device. Even though the polyacryamide coating process is expected to decrease surface potential and surface charge density, a similar charge polarization and sample trapping pattern can be observed (with a lower efficiency) by applying a higher operating potential. The lower efficiency can be overcome by adopting an even lower buffer ionic strength. One of the ongoing efforts is coating the channel with charged polymers that can reduce the amount of adsorption while maintaining the surface charge density.

Preconcentration with Buffer Additives. We have tried different nanofluidic channels with different thicknesses, as well as different buffer ionic strength. The general trend is that, the thicker the nanofluidic channel is, the lower the buffer ionic strength required for operation of the nanofluidic preconcentrator. Even a complex solution directly from the in-gel digestion of gel electrophoresis (which has high ionic strength and contains some organic solvents) can be used as sample buffer. The complex solution described in the Experimental Section was used as a "sample buffer" by adding labeled GFP molecules. For the preconcentration step, this simulated sample solution was diluted with 10 mM phosphate buffer (1:9 ratio) and loaded into the channel. In addition, various samples including proteins (Figure 3), synthesized peptide (Figure 4), fluorescent dye, and fluorescent beads were tested. In all of these cases, the trapping mechanism shown in Figure 2 can be established, while the speed of the preconcentration at different conditions varied. The adaptability of this system opens up the possibility of using samples directly from gel electrophoresis or other conventional purification techniques (using high ionic strength buffers) in the preconcentration device. Further characterization of optimized preconcentration conditions is needed for different buffer conditions. Furthermore, the size and number of the nanofilter seem to affect the concentration efficiency of the device due to different electrical field distributions in the system.

Preconcentration Coupled with On-Chip Free Solution Electrophoresis. The molecular trapping in the preconcentration device can be turned off by removing E_n. The buffer solution is expected to reestablish the ionic balance as soon as the field is turned off. When the field was turned off, the collected peak was instantly dispersed to about twice the original peak width, but there was no further dispersion observed. This dispersion reached a steady state within ~10-s time flame. As a result, the molecular plug generated by the preconcentrator can be easily manipulated either by the electric field (electrophoresis) or by the pressure-driven flow. In our design, by manipulating the field shown in Figure 4A, we can launch the molecular plug by E_T along the top microfluidic channel. Figure 4D shows the free solution electrophoresis of two protein species collected by the preconcentrator. This clearly shows the ability to couple this preconcentration device with downstream analysis, in this case, on-chip free solution electrophoresis.

CONCLUSION

This device can be fabricated with standard photolithography and etching techniques, without the need for high-resolution lithography or special fabrication tools. The ion-selective membrane in this device is the nanofluidic channel with the silica surface, which is chemically and mechanically far more robust than any other nanoporous membrane materials. Unlike frits or photopatterned nanoporous membranes with random pore size, these microfabricated nanochannels have a uniform pore size and shape, which is probably the reason for stability of the electrokinetic trapping barrier. The preconcentration factors and collection speed achieved in this device are close to those of the PCR for nucleic acid, which is an essential step for many genomics techniques. Even though this technique does not increase the number of molecules as in PCR, it collects molecules from a relatively large (~1 μL or larger) sample volume and concentrates them into a small (1pL−1nL) volume. Such a concentrated sample plug can then be efficiently sorted, separated, or detected by various microfluidic systems without sacrificing the overall detection sensitivity caused by the small sample volume capacity of microfluidic biomolecule sorting/detection systems. Therefore, the preconcentrator will act as an ideal world-to-chip (pipet-to-microchip) coupling adapter. The preconcentration device would be equivalent to the "amplifier" of the (molecular) signal in the electronic circuits, which would allow better signal processing (separation and purification, in this case). Since one could increase the signal intensity significantly (by preconcentrating molecules) just prior to detection, one could allow more aggressive biomolecule sorting or removal of high-abundance proteins without sacrificing the detectability of the minor proteins or peptides. The availability of a protein sample concentration system will allow one to use several nonlabeling detection techniques (UV absorption, for example) in the μTAS engineering, which was not possible due to the short path length and small internal volume of conventional microfluidic channels. Therefore, a combination of microfluidic biomolecule sorting and preconcentration would be an ideal platform for integrated microsystems for biomarker detection, environmental analysis, and chemical−biological agent detection.

ACKNOWLEDGMENT

This work was partially supported by NSF-CTS division (CTS-0347348, CTS-0304106), as well as MIT Lincoln Laboratory (ACC-353), MIT Ferry fund, and MIT Computational and Systems Biology initiative (CSBi). Microfabrication of the device was done in the Microsystems Technology Laboratories of MIT, with the help of its staff members.

(27) Paul, P. H.; Arnold, D. W.; Rakestraw, D. J. *Micro Total Anal. Syst.* **1998**, 49−52.
(28) Ramos, A.; Morgan, H.; Green, N. G.; Castellanos, A. *J. Phys. D* **1998**, *31*, 2338−2353.
(29) Ajdari, A. *Phys. Rev. E* **2000**, *61*, R45−R48.
(30) Hjerten, S. *J. Chromatogr.* **1985**, *347*, 191−198.

SUPPORTING INFORMATION AVAILABLE

(1) A figure showing the breakthrough of the virtual biomolecule barrier under a nonoptimized condition, $V_S = 20$ V, $V_D = 9$ V, and $V_{B1} = V_{B2} = 0$ V. The chaotic pattern indicated by the arrow demonstrates the existence of induced space charge layer and electroosmosis of the second kind. (2) A video clip is also available under the same condition. (2× the real time). This material is available free of charge via the Internet at http://pubs.acs.org.

Received for review February 21, 2005. Accepted May 27, 2005.

AC050321Z